A Study of Strong Thermal Interactions between a Laser Beam and an Absorbing Gas

RICHARD A. CHODZKO* AND SHAO-CHI LIN†
University of California, San Diego, La Jolla, Calif.

A recent study of temperature-dependent absorption, nonsteady beam propagation, and laminar to turbulent transition in a laser-induced convection column is described. The column is generated by passing a CO_2–N_2 laser beam vertically through a CO_2 absorption cell. The radial intensity distribution of the transmitted beam is scanned during the transient and quasi-steady-state absorption periods using a Ge:Au detector. During the transient period, relaxation and beam divergence effects are observed. In the quasi-steady period, a "flickering" of the beam profile from the initially Gaussian shape due to induced turbulent convection is observed at sufficiently high pressure. The onset of turbulence is measured with a fine-wire resistance thermometer and laser power meter. The transition boundary in terms of cell pressure p and incident laser power P_0 at a fixed beam diameter and cell pressure is found to be given approximately by p^2P_0 = const. This can be shown to imply a constant transition Reynolds number for the induced flow under certain restrictive conditions. The transition Reynolds number so determined is found to be surprisingly low. Local gas temperatures measured near the edge of the laser beam indicate very strong absorption heating within the convection column at the lower cell pressures.

I. Introduction

THE effects of strong interaction between a laser (or any other strong electromagnetic) beam and an absorbing atmosphere are of interest in aerospace sciences not only because they are directly related to such obvious problems as long-range communication and power transmission to distant spacecrafts, but also because better understanding of these interaction effects may lead to new terrestrial engineering applications. For example, the thermal effect of absorption may be utilized for opening up of glide paths around foggy airports, and the effect of strong localized convection within the absorption column may well be utilized for dispersal of hazardous airplane vortices and wakes through enhancement of momentum exchange and turbulent mixing. In areas of environmental control and meteorology, it is quite conceivable that the same induced convection effects from very high-power lasers could be utilized for breaking up of inversion layers and for local rain making (e.g., through enhancement of water droplet coalescence rate in otherwise stably stratified cloud layers).

Until recently, experimental laser interaction studies in absorbing gases have been concentrated in the low pressure region (typically, 1 torr or less) where relaxation phenomena are important, with the object of measuring molecular rate constants.[1,2] There has been theoretical work on the propagation of a laser beam in an absorbing gas, but usually the assumption of a constant absorption coefficient is made. Optical-acoustic coupling of a laser beam in an absorbing gas and the associated instabilities have been discussed extensively by Brueckner and Jorna,[3] and by Raizer.[4]

Presented as Paper 70-800 at the AIAA 3rd Fluid and Plasma Dynamics Conference, Los Angeles, Calif., June 29–July 1, 1970; submitted July 16, 1970; revision received December 17, 1970. This research was supported by the Advanced Research Projects Agency of the Department of Defense and was monitored by the U.S. Army Research Office-Durham, Durham, N.C., under Contract DA-31-124-ARO-D-257.

* Graduate Student, Department of Aerospace and Mechanical Engineering Sciences; currently, Member of the Technical Staff, Aerospace Corporation, El Segundo, Calif. Member AIAA.

† Professor of Engineering Physics. Associate Fellow AIAA.

An important effect due to localized heating by absorption of a laser beam is thermal defocusing. This is simply a beam divergence due to the refractive index of the medium increasing from the beam center. Gordon et al.[5] in 1965 did an early experimental and theoretical study of thermal defocusing and obtained a transient and steady-state heat conduction solution for a Gaussian beam intensity profile as a heat source in a cylindrical geometry, assuming a constant absorption coefficient. The theoretical results compared successfully with their experiments on thermal defocusing in liquids. These solutions do not apply to an absorbing gas for three reasons, 1) density variations caused by absorption heating is much more pronounced in a gaseous medium than in a liquid, 2) the convection term in the energy equation is generally not small compared to the conduction term, and 3) the temperature dependence or beam intensity dependence of the absorption coefficient is often quite strong and hence must also be taken into account. Recently D. C. Smith[6] has observed thermal defocusing effects in absorbing gases, including the forced convection effect of cross winds on beam distortion. Most recently, thermal blooming of a 10.6-μ laser beam in CO_2 has also been observed by Kenemuth, Hogge, and Avizonis.[7] Again, only the case of constant absorption coefficient has been treated in the corresponding analyses.

Another interesting thermal interaction effect is the possible onset of hydrodynamic instabilities in laser-induced convective flows. For example, the existence of strong temperature gradients due to localized heating may give rise to strong buoyancy forces. These, in turn, may cause the onset of turbulent motion within the induced convective flow. Little research has been done up to now on laser-induced convective instabilities in absorbing gases and on the problem of transition from laminar to turbulent flow as a result of such instabilities. There has been theoretical work on the scattering of a laser beam due to randomly distributed density inhomogeneities by Imai et al.[8] and by Sutton,[9] but the nature of the turbulence is specified a priori.

In this paper, some interesting results from a series of exploratory studies by the authors on strong thermal interactions between a laser beam and an absorbing gas are presented. In these studies, only constant pressure absorption heating is considered in the interaction process (that is, in

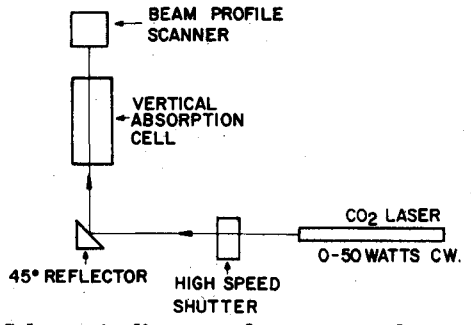

Fig. 1 Schematic diagram of experimental arrangement for measurement of radial intensity distribution of transmitted laser beam through an absorbing gas.

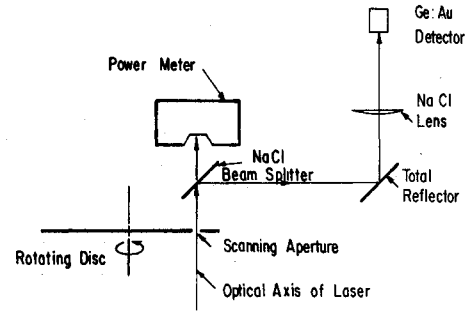

Fig. 3 Schematic diagram showing some details of radial beam profile scanner used in experimental arrangement of Fig. 1.

time scales long compared to the time required for acoustic waves to propagate out of the absorption region) but nonlinear effects such as temperature-dependent absorption and induced convection are taken into account. Because of space limitations, the results are presented in rather abbreviated forms. More detailed description of the experiments and further discussion of the results can be found in Ref. 10.

II. Experimental Arrangements

The experimental arrangements employed in the present investigation are schematically illustrated in Figs. 1 and 2. As illustrated in Fig. 1, a self-manufactured CO_2–N_2 laser which produces up to 45 watts (w) of CW power near 10.6-μ wavelength is mounted horizontally on a granite block. The TEM_{00} mode[11] with a Gaussian intensity distribution is selected out of the laser by using a long radius resonator geometry consisting of a total reflector of 10-m radius of curvature, a flat partially reflecting Germanium output coupler, and a 1.6-m separation distance between the mirrors; and by using a small 9-mm-diam discharge tube. The TEM_{00} mode is the simplest and a rather desirable beam shape for observing interaction effects on laser propagation. The Gaussian half width of the beam b, as defined by

$$I(r)/I(0) = \exp(-r^2/b^2) \quad (1)$$

measured near the exit plane of the absorption cell (with no absorbing gas in the cell) is approximately 1.5 mm and is somewhat smaller than the value of 2.5 mm predicted from laser resonator theory.[11] This is due to the fact that the Germanium output coupler acts as a positive lens due to absorption heating effects in the crystal. The small convergence angle is found to be approximately 0.25 mrad at 40-w power output and has little effect on the experimental results since it is a known constant for a given power level.

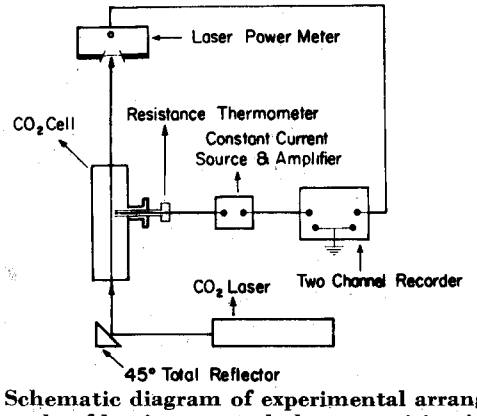

Fig. 2 Schematic diagram of experimental arrangement for the study of laminar to turbulent transition in laser-induced convection column.

The most difficult problem in obtaining experimental data is the lack of stability of the laser. By carefully cooling the laser mirrors and discharge tube and by detuning the mirrors slightly off maximum power, power meter readings remain constant to within 5% over a period of 1 hr and intensity readings using a Ge:Au detector show 5% peak to peak fluctuation with periodicity in the 1 to 10 msec range. The absorption cell is a stainless steel tank of 19 cm i.d. and 104 cm length. The 5-cm-diam sodium chloride windows mounted on the end flanges are transparent to the 10.6-μ laser radiation. Pressures in the cell are measured with a thermocouple gage and a mercury U-tube manometer. The absorption cell is vacuum tight, with a leak rate of less than 1×10^{-8} cm^3/sec S.T.P. of air determined with a Veeco leak detector, but no effort was made to evacuate the system to pressures lower than 0.01 torr before filling with CO_2 gas. At 0.01 torr cell pressure, there is negligible absorption of the 10.6-μ laser radiation by the radial gas in the cell. A flange on the side of the cell allows mounting a resistance thermometer probe at an approximately midplane axial position. A 45° total reflector mounted near the entrance plane of the vertical cell deflects the beam vertically upwards. All data is recorded with a Honeywell model 7600 FM magnetic tape recorder.

The scanning system for measuring the radial intensity distribution of the laser beam corresponding to the arrangement in Fig. 1 is shown in Fig. 3. It consists of a 12-in.-diam thin rotating disk with small holes drilled near the circumference. The hole diameter is 1 mm and therefore considerably smaller than the diameter of the transmitted laser beam. As a hole traverses the laser beam cross section in the tangent plane containing the optical axis of the beam, the emerging infrared rays are focused by means of a sodium chloride lens of 5-in. focal length onto a Philco GPC-201A Ge:Au photo-conductive detector. From the known rotational speed of the disk, the detector signal voltage vs time can be related to the intensity vs radial distance of the laser beam. In interpreting the results it is assumed that the detector signal vs time is directly proportional to the laser beam intensity vs radial distance. As seen in Fig. 3, a sodium chloride beam splitter is provided to attenuate the flux into the Ge:Au detector and to allow for calibration with a Coherent Radiation Laboratories model 201 laser power meter. The maximum power incident on the 1-mm-diam sensitive area of the detector is less than 20 mw. In measuring intensity profiles, two types of scanning disks are used depending on the required data acquisition rate, a single hole disc which produces a scan pulse every 20 msec for the standard 50 rps rotational speed, and an 18 hole disk (equally spaced and concentric) which produces a pulse every 1.1 msec. The two types of beam intensity profiles of interest are "vacuum" profiles measured at 0.01 torr cell pressure for reference purposes and "absorption" profiles measured at a specified cell pressure of CO_2 greater than 0.01 torr.

The transient data are obtained by means of a high-speed electromagnetic shutter that opens in the order of 50 μsec.

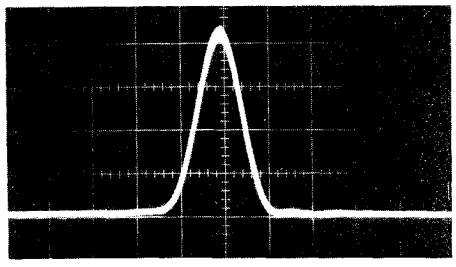

Fig. 4 Time exposure (100 scans over a 2-sec period) of beam profile scanner output with absorption cell under "vacuum condition" showing stability of laser output P_0 at 35-w level. Vertical scale: 0.5 v/cm division. Horizontal scale: 50 μsec/cm division.

The shutter essentially consists of a thin aluminum foil connected to a low-inductance condenser bank discharge circuit through an Ignitron switch. The opening action of the shutter is initiated by the self-pinching effect of the current sheet through the foil. Thus at a given cell pressure of CO_2, the beam is blocked by the shutter, the tape recorder is turned on, the shutter is fired and the transient intensity profiles are recorded.

In the arrangement shown in Fig. 2, total power transmission measurements are made using the power meter with the scanning disc removed. The resistance thermometer is mounted inside the cell at midplane and approximately 5 mm from the beam axis. The resistance thermometer is a fine platinum wire, 5 μ in diameter and 1.25 mm long, operating in a constant current, low overheat mode. Thus, the temperature fluctuation of the convection column near the edge of the beam can be simultaneously monitored with the total transmitted laser power. The operating current of the resistance thermometer is 0.6 ma and the maximum frequency response is approximately 350 cps. The output signals from the power meter and resistance thermometer are simultaneously recorded on a dual-channel strip chart recorder. The resistance thermometer is calibrated with a thermocouple and a constant temperature oven.

III. Experimental Results

Figure 4 shows a 2-sec time exposure (~100 scans) of a vacuum profile for a 35-w incident power using the single hole scanning disc. The laser is sufficiently stable to observe interaction effects, showing amplitude fluctuations of less than 5%. The observed vacuum profile is very nearly that of a TEM_{00} mode, with a Gaussian half-width $b \approx 1.5$ mm, and an intensity distribution that can be represented approximately by Eq. (1).

Figures 5 and 6 show 2-sec time exposures of the quasi-steady-state profiles for the transmitted beam at cell pressures of 40 torr and 388 torr, respectively. Thus at the lower pressure, the profile maintains a Gaussian shape of nearly the same half-width as the vacuum profile, but the absorption is much stronger than that corresponding to the room temperature absorption coefficient of 2×10^{-3} cm^{-1} for CO_2 at 10.6-μ wavelength.[10,11] On the other hand, at the

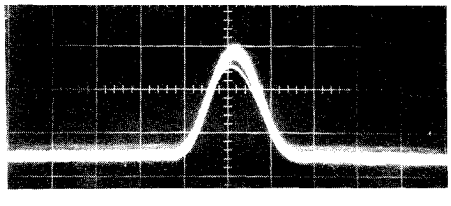

Fig. 5 Time exposure (100 scans over a 2-sec period) of quasi-steady transmitted beam profile at 40 torr absorption cell pressure and 35-w incident beam power. Vertical scale: 0.1 v/cm division. Horizontal scale: 50 μsec/cm division.

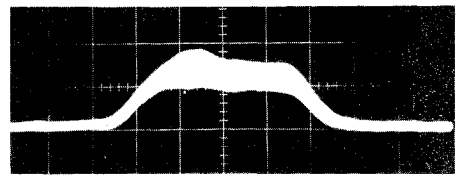

Fig. 6 Time exposure (100 scans over a 2-sec period) of quasi-steady transmitted beam profile at 388 torr absorption cell pressure and 35-w incident power. Vertical scale: 0.1 v/cm division. Horizontal scale: 50 μsec/cm division.

higher pressure, the radial intensity distribution is much wider and shows a strong time-dependent distortion from the Gaussian or a "flickering" behavior. An effective half-width b_e, which reduces to the half-width b for a Gaussian beam, can be defined as

$$\pi b_e^2 I_0 = \int_0^\infty I(r) 2\pi r dr \qquad (2)$$

where I_0 is the peak profile intensity and r the radial distance. Applying this definition to Fig. 6, a ratio of 3 between the effective half-widths of the absorption and vacuum profiles is observed. This beam divergence is due either to thermal defocusing, turbulent scattering or the combined effect of both. The "flickering" suggests that turbulent convection exists in the cell, while the large absorption at the lower pressure shows that the temperature dependence of the absorption coefficient of CO_2 gas plays an important role in the interaction.

Figure 7 is a time exposure of the transient intensity profiles at a cell pressure of 40 torr and incident power of 31 w using the single hole scanning disc. A plot of $\log(I_0/I)$ vs time is shown in Fig. 8 where I_0 is the peak intensity of the corresponding vacuum profile and I is the transient peak intensity. Thus a single relaxation time of 80 msec is observed from the linear slope of such a plot, which persists up to about 100 msec. At this pressure and incident power, the absorption heating time, assuming the vibrational states are in equilibrium, is about 2 msec. A time scale for the establishment of the laser-induced convection column is estimated to be 13 msec (see Chap. IV, Sec. F in Ref. 10). The observed time scale τ_1 is much longer than either of the preceding and is therefore interpreted to be a vibrational relaxation effect. From Fig. 7, the transient interaction of 40 torr shows little defocusing or beam distortion from the initial Gaussian profile. Figure 9 is a plot of intensity vs radial distance at various times taken from a time exposure of the transient intensity profiles at a cell pressure of 730 torr and an incident beam power of 36 w using the 18 hole scanning disk. The fact that the initial pulse corresponds to $I/I_0 \approx 0.78$ shows that it must have occurred near $t = 0$ since the room temperature coefficient gives $I/I_0 \approx 0.8$. The time $t = 0$ is uncertain to within the time between scans of 1.1 msec. A plot of $\log(I_0/I)$ vs time is shown in Fig. 10 and it is seen that two characteristic times are in evidence. The dotted and dash-dotted lines are both empirical fits of the

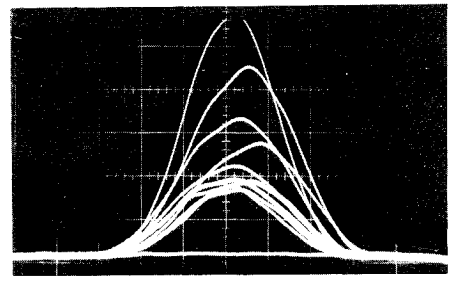

Fig. 7 Time exposure of beam profile scanner output during transient absorption period (50 scans/sec) at 40 torr cell pressure and 32-w incident power.

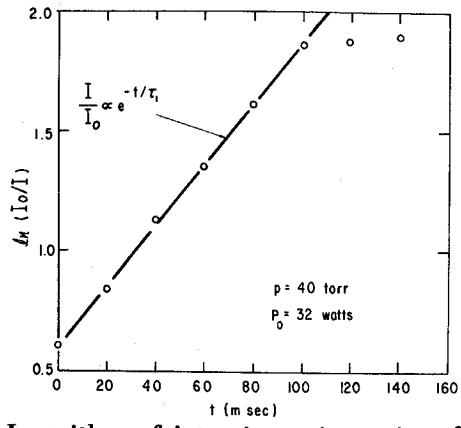

Fig. 8 Logarithm of intensity ratio vs time for transient data illustrated in Fig. 7. (I = instantaneous peak-intensity during transient absorption period; I_0 = peak intensity of corresponding "vacuum" profile.)

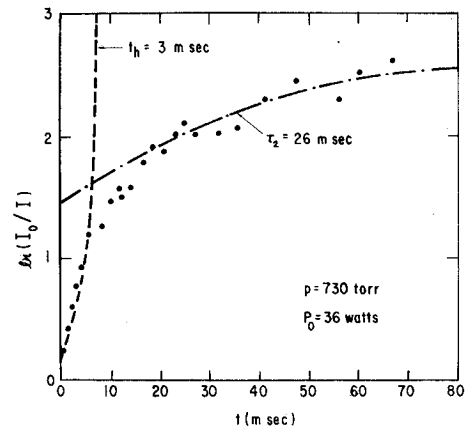

Fig. 10 Logarithm of intensity ratio vs time from transient data illustrated in Fig. 9. The dotted line is a fit of the data with a constant pressure heating theory, giving a 3-msec time scale t_h. The dash-dotted line is an empirical fit of the data giving a saturation relaxation time scale τ_2 of 26 msec.

data, giving 3 msec t_h and 26 msec τ_2 time scales, respectively. Figures 9 and 10 suggest that at 730 torr pressure, the interaction process occurs in two phases: 1) an initial phase where weak localized heating due to absorption creates radial density gradients and thus thermal defocusing while maintaining a nearly Gaussian intensity profile and 2) a final slower phase where localized heating, conduction, and induced convection produce a further beam divergence as well as significant distortion from the initial Gaussian distribution. The radial beam profiles in Fig. 9 were integrated over the beam area and it was found that the total transmitted beam power is nearly constant for the first few msec. This indicates that only relatively weak absorption has taken place during the observed 3 msec time scale t_h.

A plot of percent transmission vs cell pressure at various incident power levels using the power meter is shown in Fig. 11. Drift in the laser power output, calibration accuracy of the power meter and errors in making measurements limit the accuracy of these results to about 15%, but the general trends are not in doubt. It is seen that at low power levels (of the order of 1 w), the percent transmission is nearly independent of pressure above the collision broadened limit (which occurs at approximately 10 torr[12]) and agrees within 10% of the room temperature absorption coefficient. At power levels of the order of 5 w, a dip in the transmission begins to appear in the vicinity of 40 torr, which seems to indicate that the temperature dependence of the absorption coefficient is just becoming important at this power level. At 38 w, a minimum percent transmission of about 15% is observed at 35 torr increasing to 65% at 1 atm. These general trends are consistent with a simple laminar convection solution[19] discussed in the next section, in that the gas temperature rise is inversely proportional to the cell pressure and that the absorption coefficient increases with temperature. In measuring the transmission curves, it was observed that for sufficiently high power levels the power meter readings showed large random fluctuations over and above the inherent laser noise and the percent transmission is based upon a time average over the fluctuations. This again indicates that the induced convection is turbulent.

To verify the existence of turbulence, simultaneous power meter and resistance thermometer measurements were made with the experimental arrangement illustrated in Fig. 2 and described previously in Sec. II. The cell pressure p is varied from a few torr to atmospheric pressure, with the laser set at a fixed incident power level $P_0 = \pi b^2 I_0$ ranging from 1 to 40 w.

The experimental results of the transmitted laser power and gas temperature measurements are shown in Figs. 12 and 13. Figure 12 shows some typical strip chart records of the power meter and thermometer signals at incident laser power levels of 30 w, 13 w, and 3 w, respectively. These records were obtained by tuning the laser to run stably at the desired output power level and let the beam pass continuously through the vertical absorption cell. The stability of the laser output is first checked by keeping the cell at the "vacuum condition" as previously defined for a sufficiently long period of time

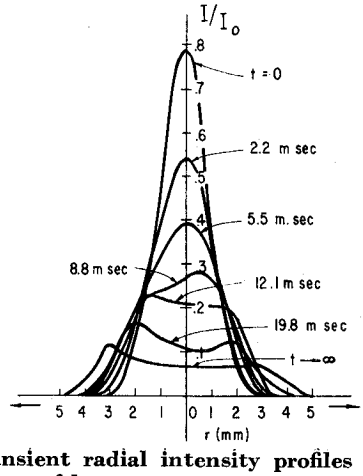

Fig. 9 Transient radial intensity profiles plotted from time exposure of beam scanner output during transient absorption period at a scanning rate of 900 scans/sec for an incident beam power of 36 w and 730 torr cell pressure of CO^2. (I_0 = peak centerline intensity of corresponding "vacuum" profile.)

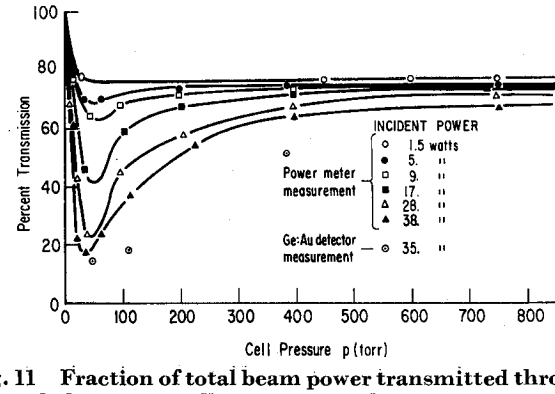

Fig. 11 Fraction of total beam power transmitted through vertical absorption cell measured with power meter vs cell pressure at various incident beam power levels. (Pressure readings accurate to ±1 torr; power meter readings accurate to ±15%.)

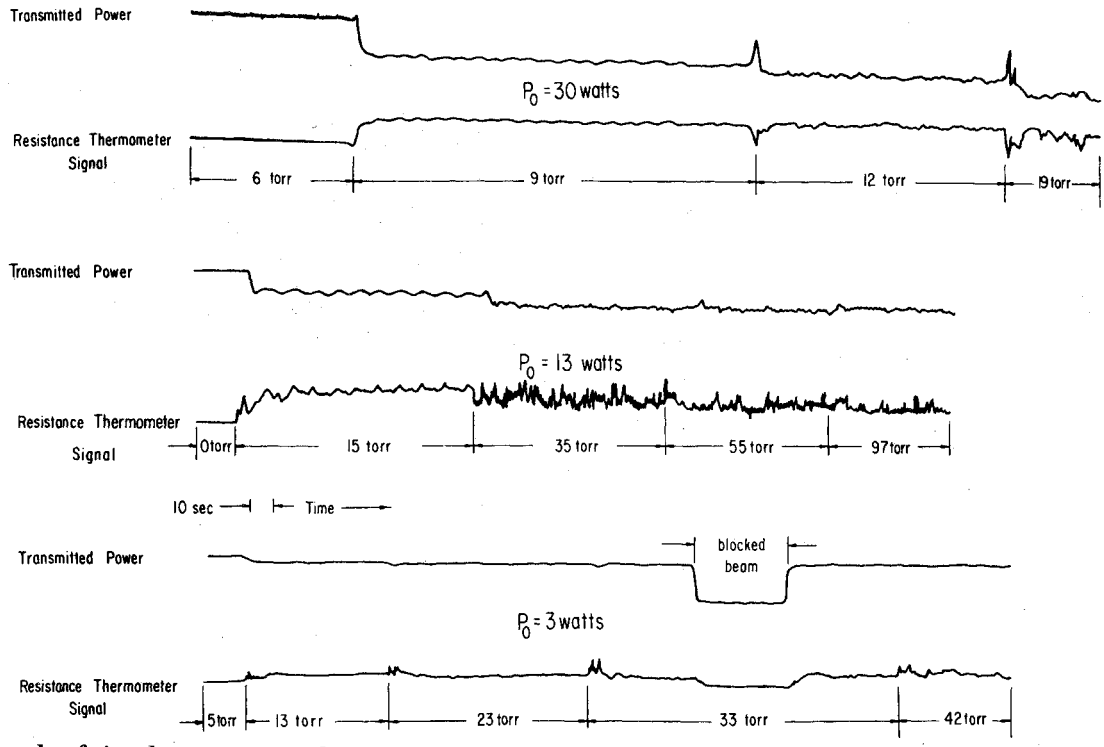

Fig. 12 Sample of simultaneous strip chart recording of transmitted laser beam and fine wire thermometer signals at three different incident beam power levels showing the effects of changing absorption cell pressure. Increasing randomness of temperature fluctuation with increasing pressure as measured from fine wire probe located inside the absorption cell 5 mm from the optical axis of the laser beam suggests transition from laminar to turbulent flow in the laser-induced convection column.

(typically, of the order of several minutes). Then a small amount of CO_2 gas is let into the absorption cell by a quick opening of the gas inlet valve, and the filling pressure p is subsequently allowed to settle down to some low constant value (of the order of a few torr) while the power meter and the thermometer signals are being continuously recorded for a certain period of time (typically, of the order of a minute). The filling pressure is then increased in successive steps by repeating the process of admitting more gas, pressure relaxation, and quasi-steady-state recording. (It may be noted that the pressure relaxation time is roughly determined by the acoustic reverberation time over the longest dimension of the cell, and hence quite immaterial in comparison with the manual manipulation time of the gas inlet valve during the pressure changing step.)

From the top pair of the strip chart records shown in Fig. 12, it is seen that at an incident power of 30 w, both the transmitted power and temperature signals appear very quiet when the cell pressure is kept at the 6 torr level. When the cell pressure is increased to 9 torr, the recorded signals begin to display an oscillatory behavior. It is interesting to note the approximately sinusoidal signals concurrently from both the power meter and the thermometer at the latter cell pressure. As the cell pressure is increased further to 12 and 19 torr, the signals take on a more and more random character. The thermometer voltage fluctuations at 40 torr correspond to peak-to-peak temperature fluctuations of the order of 20% of the local mean temperature $\bar{T} \cong 500°K$. The fact that such high gas temperatures were observed at a radial distance $r = 5$ mm (i.e., about 3 times the Gaussian half-width b of the laser beam) from the beam center indicates that very strong gas heating must be taking place within the absorption column.

From the middle pair of strip chart records shown in Fig. 12, it is seen that the same type of behavior is observed at 13 w with the onset of instability occurring at somewhat higher pressure. The frequency response of the resistance thermometer is of course much greater than that of the power meter (about 350 Hz vs 10 Hz). This difference is reflected in the higher harmonic content of the thermometer signal at

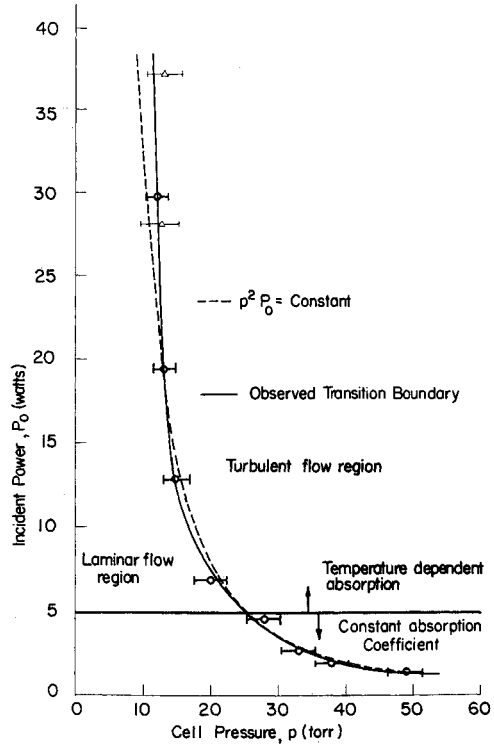

Fig. 13 Transition boundary from laminar to turbulent flow in laser-induced convection column in terms of incident CO_2 laser power and CO_2 absorption cell pressure and comparison with p^2P_0 = constant curve.

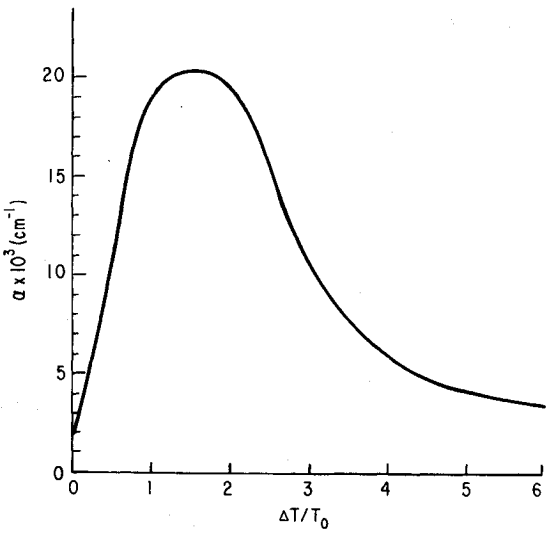

Fig. 14 Theoretical temperature dependence of the absorption coefficient of CO_2 gas at 10.6-μ wavelength. (Numerical value taken from Ref. 14. $\Delta T \equiv T - T_0$ where $T_0 = 300°K$.)

the higher pressures. The power meter and resistance thermometer signals corresponding to zero cell pressure provide a means of comparison with the fluctuations and show the relative low inherent laser noise. At 3-w incident power, Fig. 12 shows an essentially quiescent signal from the power meter for the entire range of pressures. The resistance thermometer signal, on the other hand, continues to show increasing fluctuation with increasing absorption pressure. Thus, at this low power level, the transmitted power and gas temperature are essentially "de-coupled" in the sense that the temperature fluctuations are too small to affect the absorption through the temperature dependence of the absorption coefficient. The magnitude of the temperature fluctuations are measured to be of the order of 0.1% at the 3-w incident power level.

The general trend of increased randomness of both the power meter signal and the fine wire thermometer signal (especially the latter) with increasing absorption cell pressure at any given incident power level can therefore be interpreted as being caused by a fluid dynamic transition from laminar to turbulent flow within the laser-induced convection column. It is interesting to note that such transition appears to be quite sharp, since a marked increase in temperature fluctuation amplitude as well as in randomness of the fluctuating signal when the cell pressure is increased by a factor of about 2 is quite evident. In Fig. 13, we show the "transition boundary" generated by making a series of the preceding type of measurements at various incident power levels. The transition point at a given power level is defined by the pressure at which the resistance thermometer signal becomes noticeably random. It is interesting to note that the transition boundary can be fitted closely over the measured range of incident power levels, by a curve $p^2P_0 = \text{const}$.

IV. Theoretical Interpretation

The laser interaction process in an absorbing gas is described by the source-free Maxwell's equations coupled with the appropriate fluid conservation equations.[3,4,13] The interaction equations as formulated by Akhmanov et al.[13] were derived within the eikonal approximation assuming that the electric field amplitude and phase were slowly varying functions of the axial coordinate z and rapidly varying functions of the radial coordinate r; that the dielectric constant was a function only of temperature; and that the absorption coefficient was a constant. If the absorption coefficient is a function of temperature, but the latter is only a slowly varying function of the spatial coordinates (i.e., in length scales of the order of the incident wavelength), such formulation should remain approximately valid. Accordingly, we let

$$E(r,z,t) = E_0(r,z) \exp\{i[\omega t - kz - kS(r,z)] - \alpha z/2\} \quad (3)$$

where E_0 is the local field amplitude, ω is the radian frequency of the incident radiation, k is the wave number, S is the phase factor and $\alpha = \alpha(T)$ is the power absorption coefficient. If Eq. (3) is substituted into the wave equation as implied by the source-free Maxwell's equations and making the preceding approximations, one gets

$$q\partial(E_0^2)/\partial r + E_0^2(q/r + \partial q/\partial r) + \partial(E_0^2)/\partial z + \alpha E_0^2 = 0 \quad (4)$$

$$q\partial q/\partial r + \partial q/\partial z = -(1/n)(\partial n/\partial T)\partial T/\partial r \quad (5)$$

where $q \equiv \partial S/\partial r$ is a parameter which defines the inclination of the ray paths with respect to the z axis (e.g., $q = 0$ implies axial rays or no beam divergence), and n is the index of refraction. If convection effects are neglected, the fluid properties are related to the field by

$$\rho C_p \partial T/\partial t = \nabla\cdot(K\nabla T) + \alpha(T)I = 0 \quad (6)$$

where $I \equiv (c/8\pi)E_0^2$ is the local beam intensity.

For the case of $q \ll 1$, Eq. (4) can further be approximated by

$$\partial I/\partial z + \alpha(T)I = 0 \quad (7)$$

By solving Eqs. (6) and (7) for $I(r,z,t)$, i.e., assuming $q = 0$, the defocusing effect can be calculated for small beam divergence angles in an iterative manner as was done by Gordon et al.[5] The theoretical temperature dependence of α for CO_2 gas at the 10.6-μ laser wavelength assuming equilibrium population of the vibrational-rotational states, a P-branch $J = 20$ transition, and collision-broadened lines[12,14,15] is approximately that shown in Fig. 14. According to Ref. 12, the collision-broadened line assumption should be valid down to about 10 torr pressure near room temperature. On the other hand, the conditions under which the equilibrium assumption remains valid is governed by kinetics considerations.[16] Even though this latter assumption is very much in doubt in the lower pressure range of the present experiments,[10] it is nevertheless interesting to examine the localized absorption heating effects within this simple assumption. Thus, according to Fig. 14, the dependence of α on T is very strong, with a maximum value at $T \cong 750°K$ which is about 10 times the room temperature value $\alpha_0 \cong 2 \times 10^{-3}\ \text{cm}^{-1}$.

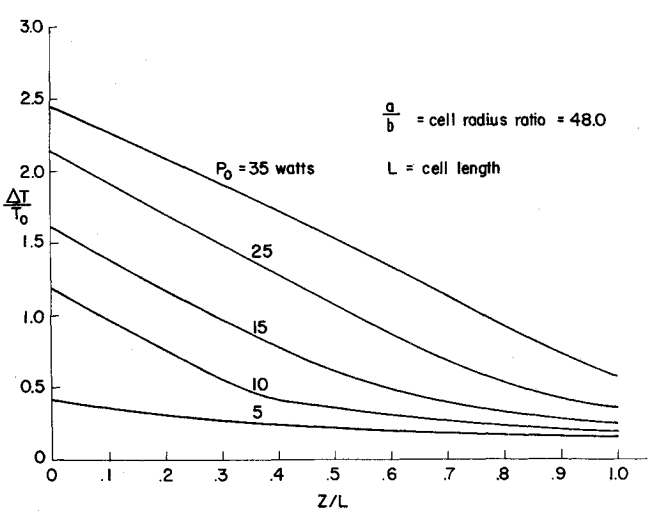

Fig. 15 Theoretical calculation of centerline temperature vs axial distance at various incident power levels from steady-state conduction solution.

The heat conduction coefficient K is a rather mild function of temperature and insensitive to the rate processes. Within the temperature range of interest here, it can be approximated by[17] $K/K_0 \cong (T/T_0)^{0.9}$, where $K_0 = 4 \times 10^{-5}$ cal (°K-cm-sec)$^{-1}$, and $T_0 = 300$°K.

To obtain an upper limit on the initial rate of increase of gas temperature or beam absorption, one can solve Eq. (6) with the conduction term neglected. Assuming a linear temperature dependence of the absorption coefficient where the initial slope is determined from Fig. 14, one gets

$$\rho C_v \partial T/\partial t = \alpha_0[1 + \beta(T - T_0)/T_0]I \tag{8}$$

with $\beta \equiv d(\alpha/\alpha_0)/d(T/T_0) \cong 10$.

A solution to Eq. (8) can be obtained by neglecting the variation of the intensity with temperature, i.e., neglecting the effect of beam intensity reduction with increasing absorption due to increased temperature. This again establishes an upper limit. For the case of heat addition at constant pressure, $p = \rho RT$, with $T = T_0$ at $t = 0$, the solution, valid for $\beta > 1$, is

$$\frac{\alpha(t)}{\alpha_0} = 1 + \beta\frac{\Delta T(t)}{T_0} = \frac{(\beta - 1)\exp(t/t_h)}{\beta - \exp(t/t_h)} \tag{9}$$

where

$$t_h = p\gamma/[(\gamma - 1)(\beta - 1)\alpha_0 I_0] \tag{10}$$

is the characteristic equilibrium heating time based on the peak intensity of the incident beam. The specific heat ratio $\gamma \equiv C_p/C_v$ for CO_2 is approximately 1.25 over the temperature range of interest.

The transmitted beam intensity through the absorption cell of length L is given by

$$I = I_0 \exp\left(-\int_0^L \alpha dz\right) \geq I_0 \exp(-\alpha_{\max} L) \tag{11}$$

where $\alpha_{\max}$ is now the time-dependent beam-center absorption coefficient near the entrance plane as calculated in accordance with Eq. (9). From Eq. (11), we obtain

$$\log(I_0/I) \leq \alpha_0 L(\beta - 1)\exp(t/t_h)/[\beta - \exp(t/t_h)] \tag{12}$$

Thus, the initial slope of $\log(I_0/I)$ should be approximately given by $\alpha_0 L/t_h$ for $t \ll t_h$. A comparison of the experimental data in Fig. 10 with Eq. 12 gives a reasonably good fit for $t_h = 3$ msec near $t = 0$ as illustrated by the dotted curve. From the peak incident beam intensity $I_0 = 500$ w/cm^2, the value of t_h computed for the preceding transient profiles at $p = 730$ torr, $P_0 = 36$ w should be approximately 50 msec. Since the time scale so calculated should correspond to an upper bound for the heating rate, the observed initial rate of attenuation of transmitted beam intensity is much more rapid than expected. The extents to which thermal defocusing and/or nonequilibrium population of the $CO_2(01°0)$ absorbing state may have contributed to the apparent acceleration of the rate of beam centerline intensity attenuation have not yet been determined. One possible source of experimental error could be a nonlinear Ge:Au detector response. This is not believed to be a likely contributor to the observational discrepancy since any saturation effect due to overheating of the Ge:Au detector should have the opposite effect of yielding a longer time constant. Furthermore, a linearity check was made by comparing the power meter transmission curves in Fig. 11 with the power transmission obtained by integration of the quasi-steady-state intensity profiles and the results agreed to within 10%.

The second time scale $\tau_2 = 26$ msec shown in Fig. 10 was obtained by assuming that the beam center intensity approaches its quasi-steady-state value $\bar{I}$ according to a simple relaxation formula

$$(I - \bar{I}) \propto e^{-t/\tau_2} \tag{13}$$

Quantitative interpretation of this time scale is likely to be complicated since it must involve the combined effects of transient heating, conduction, and convection.

Equation (6) also defines a characteristic conduction time scale

$$t_c \equiv \rho_0 C_p b^2/K = p\gamma b^2/(\gamma - 1)KT_0 \tag{14}$$

where b is the Gaussian half-width of the laser beam. Thus, by equating t_c to t_h, one can define a critical incident power level

$$P_0^* \equiv \pi b^2 I_0^* = \pi K T_0/2\alpha_0(\beta - 1) \tag{15}$$

which, when approached or exceeded, leads to strong localized heating of the gas. For pure CO_2 gas absorbing at 10.6 μ, $P_0^* \cong 5$ w.

In order to establish an upper limit to the temperature-dependent absorption and its contribution to the convective effects, the nonlinear steady-state conduction problem was solved first. The system of equations to be solved, assuming conduction in the z direction to be much less than in the r direction, consists of Eq. (6), which becomes, approximately

$$K(T)(1/r)(\partial/\partial r)(r\partial T/\partial r) + \alpha(T)I = 0 \tag{16}$$

and Eq. (7), with $I(r, 0) = I(0, 0)\exp(-r^2/b^2)$; $T = T_0$ at $r = a$, the cell radius; and $\alpha(T)$ and $K(T)$ as just given. The solution to this set of coupled nonlinear partial differential equations is obtained numerically by using a finite-difference technique with piece-wise linear approximation to the temperature dependence of the absorption coefficient.

The solution plotted in Fig. 15 shows the centerline temperature variation with axial distance for various incident laser power levels. The effect of strong localized heating for power levels above 5 w is clearly seen. The axial temperature gradients should induce strong convective effect in the vertical cell. These temperatures give an upper limit to the absorption heating effect. Convection, anharmonic corrections and dissociation effects should reduce the actual temperature to lower values. The effect of self heating in increasing the absorption with increasing incident power level above the critical value is seen and is observed experimentally in Fig. 11. It can be shown that convection (the induced flow Reynolds number) is proportional to the gas pressure; the steady-state conduction solution on the other hand is independent of pressure and consequently should be a better approximation with decreasing pressure at least until the absorption line becomes Doppler-broadened. At beam power levels of the order of 1w, the effect of the temperature dependence of the absorption coefficient is small and the solution should match the experimental results of McCubbin et al.[18] and of Gerry and Leonard.[12] This is consistent with the transmission curve of Fig. 11 which agrees with these latter experiments to within 10% in the low power limit, and also with the conduction solution of Gordon et al.[5] which assumed a constant absorption coefficient.

The radial temperature profiles at the entrance and exit planes of the cell for a 35-w beam is shown in Fig. 16. A comparison of the nonlinear steady-state conduction solution intensity profile with the experimental profiles at 48 torr and 388 torr is given in Fig. 17 for an incident power of 32 w, where the dotted line is the conduction solution neglecting thermal defocusing. It is seen that the agreement improves with decreasing pressure both in the beam shape and in the absolute magnitude of the absorption.

In contrast to the zero-flow-velocity implied in the conduction solution, an approximate steady-state convection solution can be obtained from dimensional arguments under certain restrictive assumptions.[19] The steady-state conduction solution shows the importance of the temperature dependence of the absorption coefficient in the interaction process, while the convection solution allows one to interpret the observed increase in temperature fluctuation with absorption cell pres-

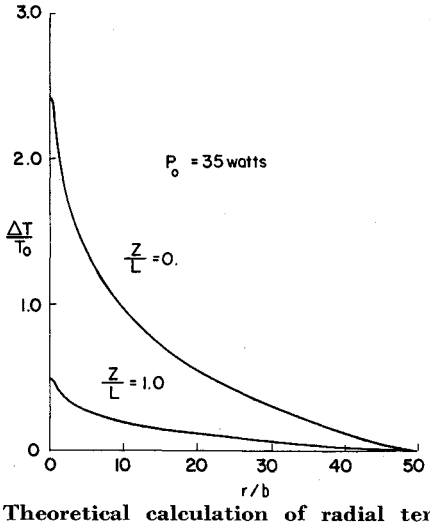

Fig. 16 Theoretical calculation of radial temperature profiles within CO_2 absorption cell at entrance and exit planes of cell from steady-state conduction solution.

sure in terms of fluid dynamic transition from laminar to turbulent flow in the absorption-induced convection column.

As we have shown in Ref. 19, an approximate convection solution based on simple dimensional arguments lead to the following expression for the induced flow Reynolds number within the vertical absorption column of effective radius r_e and length L:

$$R_e = \frac{2\bar{\rho}\bar{u}r_e}{\bar{\mu}} = \left[(p^2P_0)\left(\frac{\bar{\alpha}}{\bar{C}_p\bar{\mu}^3}\right)\frac{gLr_e^2}{6\pi R^2T_0^3}\right]^{1/2} \quad (17)$$

where $\bar{\rho}$, $\bar{\mu}$, $\bar{\alpha}$, and $\bar{C}_p$ denote, respectively, the gas density, viscosity coefficient, absorption coefficient, and specific heat evaluated at the mean temperature $\bar{T}$ within the column; $\bar{u}$ is the mean vertical induced flow velocity; g is the gravitational acceleration; and R is the gas constant. From the known temperature dependence of μ, C_p, and α for CO_2, the quantity $\bar{\alpha}/\bar{C}_p\bar{\mu}^3$ is relatively independent of temperature (i.e., with variation less than $\pm 30\%$ over the temperature range $300 < T < 700°K$). Thus, $p^2P_0 = \text{const}$ indicates a constant induced flow Reynolds number for laminar-turbulent transition as observed experimentally in Fig. 13. With this observed transition boundary, $p^2P_0 \cong 3 \times 10^3$ (torr)^2-w, substitution of numerical values into Eq. (17) then yields a transition Reynolds number $Re^* \cong 3r_e/b$. Since r_e must lie somewhere between the beam half-width b and the absorption cell radius $a \cong 60\,b$, we have $1 < (r_e/b) < 60$, so that

$$3 < Re^* < 180 \quad (18)$$

Considering the fact that the actual value of r_e/b is likely to be much closer to 1 than to 60, the transition Reynolds number thus deduced is, indeed, surprisingly low.

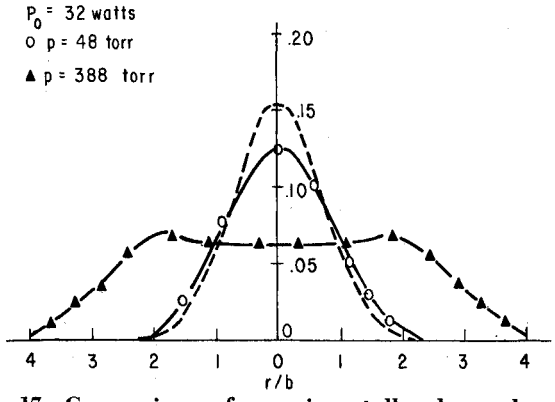

Fig. 17 Comparison of experimentally observed quasi-steady-state beam intensity profiles with theoretical radial intensity distribution predicted from steady-state conduction solution neglecting thermal defocusing (dotted curve).

References

[1] Steinfeld, J. I., et al., "Saturation of Molecular Vibrational Levels by Infrared Pumping," *Bulletin of the American Physical Society*, Ser. II, Vol. 13, No. 3, March 1968, p. 449.

[2] Moore, C. B., Wood, R. E., Hu, B.-L., and Yardley, J. T., "Vibrational Energy Transfer in CO_2 Lasers," *Journal of Chemical Physics*, Vol. 46, No. 11, June 1, 1967, pp. 4222–4231.

[3] Brueckner, K. A. and Jorna, S., "Linearized Theory of Laser Induced Instabilities in Liquids and Gases," *Physical Review*, Vol. 164, No. 1, Dec. 5, 1967, pp. 182–193.

[4] Raizer, Y. P., "Self Focusing and Defocusing, Instability and Stabilization of Light Beams in Weakly Absorbing Media," *Soviet Physics JETP*, Vol. 25, No. 2, Aug. 1967, pp. 308–316.

[5] Gordon, J. P., et al., "Long Transient Effects in Lasers with Inserted Liquid Samples," *Journal of Applied Physics*, Vol. 36, No. 1, Jan. 1965, pp. 3–8.

[6] Smith, D. C., "Thermal Defocusing of CO_2 Laser Radiation in Gases," *IEEE Journal of Quantum Electronics*, Vol. QE-5, No. 12, Dec. 1969, pp. 600–607.

[7] Kenemuth, J. R., Hogge, C. B., and Avizonis, P. V., "Thermal Blooming of a 10.6-μ Laser Beam in CO_2," *Applied Physics Letters*, Vol. 17, No. 5, Sept. 1, 1970, pp. 220–223.

[8] Imai, M., Kikuchi, S., and Matsumoto, T., "Mode Conversion Due to Fluctuations in a Lens-like Medium," *Journal of the Optical Society of America*, Vol. 59, No. 8, Aug. 1969, Pt. 1, pp. 904–913.

[9] Sutton, G., "Effect of Turbulent Fluctuations in an Optically Active Fluid Medium," *AIAA Journal*, Vol. 7, No. 9, Sept. 1969, pp. 1737–1743.

[10] Chodzko, R. A., "Thermal Interaction of a Laser Beam in an Absorbing Gas," Ph.D. dissertation, 1970, Dept. of Aerospace and Mechanical Engineering Sciences, Univ. of California, San Diego.

[11] Kogelnik, H. and Li, T., "Laser Beams and Resonators," *IEEE Proceedings*, Vol. 54, No. 10, Oct. 1966 pp. 1312–1328.

[12] Gerry, E. T. and Leonard, D. A., "Measurement of 10.6-μ CO_2 Laser Transition Probability and Optical Broadening Cross Sections," *Applied Physics Letters*, Vol. 8, No. 9, May 1, 1966, pp. 227–229.

[13] Akhmanov, S. A., et al., "Thermal Self-Actions of Laser Beams," *IEEE Journal of Quantum Electronics*, Vol. QE-4, No. 10, Oct. 1968, pp. 568–575.

[14] Penner, S. S., "Selected Applications of Laser Interactions in Applied Science," *Astronautica Acta*, Vol. 15, No. 1, Jan. 1969, pp. 1–15.

[15] Herzberg, G., *Molecular Spectra and Molecular Structure II. Infrared and Raman Spectra of Polyatomic Molecules*, 1st ed., Van Nostrand, Princeton, N. J., 1945, pp. 272–276.

[16] Taylor, R. L. and Bitterman, S., "Survey of Vibrational Relaxation Data for Processes Important in the CO_2-N_2 Laser System," *Reviews of Modern Physics*, Vol. 41, No. 1, Jan. 1969, pp. 26–47.

[17] Hirschfelder, J. Q., Curtiss, C. F., and Bird, R. B., Molecular *Theory of Gases and Liquids*, 1st ed., Wiley, New York, corrected, with Notes added, March 1964, pp. 573–574.

[18] McCubbin, T. K., Jr., Darone, R., and Sorrell, J., "Determination of Vibration-Rotational Line Strengths and Widths in CO_2 Using a CO_2-N_2 Laser," *Applied Physics Letters*, Vol. 8, No. 5, March 1, 1966, pp. 118–119.

[19] Chodzko, R. A. and Lin, S. C., "Transition from Laminar to Turbulent Flow in a Laser-Induced Convection Column," *Applied Physics Letters*, Vol. 16, No. 11, June 1, 1970, pp. 434–436.